Chapter 14
Tonga

14.1 Climate Summary

14.1.1 Current Climate

- Annual and November–April mean temperatures have increased at Nuku'alofa since 1949. Trends in Nuku'alofa annual maximum temperature and November–April maximum and minimum temperature are also positive. This is consistent with global warming.

- Annual and half-year rainfall trends show little change at Nuku'alofa and Lupepau'u with the exception of Lupepau'u May–October rainfall which has increased since 1947. Extreme daily rainfall trends show little change at Nuku'alofa since 1971 and Lupepau'u since 1947.

- Tropical cyclones affect Tonga mainly between November and April. An average of 20 cyclones per decade developed within or crossed the Tonga Exclusive Economic Zone (EEZ) between the 1969/70 to 2010/11 seasons. Nineteen of the 55 tropical cyclones (35%) between the 1981/82 and 2010/11 seasons were severe events (Category 3 or stronger) in the Tonga EEZ. Available data are not suitable for assessing long-term trends.

- Wind-waves around Tonga do not vary substantially in height throughout the year. Seasonally, waves are influenced by the trade winds and tropical storms, and display variability on interannual time scales with the El Niño–Southern Oscillation (ENSO) and Southern Annular Mode (SAM). Available data are not suitable for assessing long-term trends.

14.1.2 Climate Projections

For the period to 2100, the latest global climate model (GCM) projections and climate science findings indicate:

- El Niño and La Niña events will continue to occur in the future (*very high confidence*), but there is little consensus on whether these events will change in intensity or frequency;

- It is not clear whether mean annual rainfall will increase or decrease and the model average indicates little change (*low confidence in this model average*), with more extreme rain events *(high confidence)*;

- Drought frequency is projected to decrease slightly (*low confidence*);

- Ocean acidification is expected to continue *(very high confidence)*;

- The risk of coral bleaching will increase in the future (*very high confidence*);

- Sea level will continue to rise (*very high confidence); and*

- December–March wave heights and periods are projected to decrease slightly *(low confidence)*.

14.2 Data Availability

There are currently seven operational meteorological stations in Tonga. Multiple observations within a 24-hour period are taken at Fua'amotu, Lupepau'u, Niuatoputapu (formerly known as Keppel), Ha'apai and Niuafo'ou. A single daily observation is taken at Nuku'alofa and Kaufana. Nuku'alofa and Fua'amotu, the primary stations, are located on the northern and southern side of Tongatapu Island, respectively. Nuku'alofa has rainfall data from 1938 and air temperature data from 1945. Lupepau'u, Ha'apai and Niuatoputapu have temperature data from 1950 and rainfall data from 1940 to 1947.

Nuku'alofa monthly rainfall from 1938 (daily values from 1971) and monthly air temperature data from 1949, and Lupepau'u rainfall from 1947 and air temperature data from 1956 have been used in this report. Both records are homogeneous. Additional information on historical climate trends in the Tongan region can be found in the Pacific Climate Change Data Portal www.bom.gov.au/climate/pccsp/.

Wind-wave data from buoys are particularly sparse in the Pacific region, with very short records. Model and reanalysis data are therefore required to detail the wind-wave climate of the region. Reanalysis surface wind data have been used to drive a wave model over the period 1979–2009 to generate a hindcast of the historical wind-wave climate.

14.3 Seasonal Cycles

Information on temperature and rainfall seasonal cycles can be found in Australian Bureau of Meteorology and CSIRO (2011).

14.3.1 Wind-driven Waves

Surface wind-wave driven processes can impact on many aspects of Pacific Island coastal environments, including: coastal flooding during storm wave events; coastal erosion, both during episodic storm events and due to long-term changes in integrated wave climate; characterisation of reef morphology and marine habitat/ species distribution; flushing and circulation of lagoons; and potential shipping and renewable wave energy solutions. The surface offshore wind-wave climate can be described by characteristic wave heights, lengths or periods, and directions.

The wind-wave climate of Tonga shows small spatial variability across the region.

Near the capital, Nuku'alofa, southerly waves are blocked by the island. Throughout the year, waves are predominantly directed from the east and display little variability in height (Figure 14.1). The wave climate at Nuku'alofa is characterised by the trade winds, with swell from extra-tropical storms. During June–September, mean waves are slightly shorter than the annual mean (seasonal mean period around 7.4 s), consisting of trade wind generated waves from the east, and a south-westerly component of swell propagated from storm events in the Southern Ocean. During December–March, mean waves are slightly longer than the annual mean (seasonal mean period around 8.6s) (Table 14.1) and are directed mostly from the north-east due to locally and remotely generated trade wind waves, with some northerly swell due to North Pacific storms and cyclones. Waves larger than 2.9 m (99th percentile) at Nuku'alofa occur predominantly during December–March, directed from the north-west through to east, with large waves incident from the north-west and east in other months. The height of a 1-in-50 year wave event to the north of Nuku'alofa is calculated to be 10.6 m.

On the outlying northern islands (e.g. to the north of Lupepau'u airport), waves are characterised by variability of the Southern Hemisphere trade winds, though wave height remains fairly consistent year round (Figure 14.2). During June–September, waves near Lupepau'u are easterly and of slightly shorter than annual mean period (seasonal mean around 8.0 s). These waves consist of local trade wind generated waves, and south-east and south-west swell from Southern Ocean extra-tropical storms. During December–March, the mostly easterly waves are generated locally by trade winds, with swell waves from the south-east, north-east and north-northwest, giving a slightly longer average seasonal period (mean period around 9.1 s) (Table 14.1). Waves larger than 3.2 m (99th percentile) occur in December–March from the north-west through to the east due to tropical cyclones and extra-tropical storms, with some large easterly waves seen in the dry season, likely associated with Southern Ocean storms. The height of a 1-in-50 year wave event north of Lupepau'u is calculated to be 9.3 m.

No suitable dataset is available to assess long-term historical trends in the Tonga wave climate. However, interannual variability may be assessed in the hindcast record. The wind-wave climate displays strong interannual variability near both Nuku'alofa and Lupepau'u, varying with the El Niño– Southern Oscillation (ENSO) and slightly with the Southern Annular Mode (SAM). During El Niño years, wave power is approximately 25% greater during December–March due to movement of the South Pacific Convergence Zone (SPCZ) away from Tonga, while in June–September wave power is substantially greater during La Niña years with waves more strongly directed from the east associated with increased trade winds. When the SAM index is negative, easterly wave power is reduced due to enhanced westerly components during June–September.

Table 14.1: Mean wave height, period and direction from which the waves are travelling around Tonga in December–March and June– September. Observation (hindcast) and climate model simulation mean values are given with the 5–95th percentile range (in brackets). Historical model simulation values are given for comparison with projections (see Section 14.5.6 – Wind-driven waves, and Table 14.7). A compass relating number of degrees to cardinal points (direction) is shown.

		Hindcast Reference Data (1979–2009) – Nuku'alofa	Hindcast Reference Data (1979–2009) – Lupepau'u	Climate Model Simulations (1986–2005) – Tonga
Wave Height (metres)	December–March	1.4 (0.8–2.3)	1.7 (1.1–2.6)	1.8 (1.7–2.0)
	June–September	1.3 (0.7–2.2)	1.6 (1.0–2.5)	2.1 (1.7–2.4)
Wave Period (seconds)	December–March	8.6 (6.5–11.4)	9.1 (7.2–11.8)	8.7 (7.8–9.6)
	June–September	7.4 (5.7–9.8)	8.0 (6.5–10.3)	8.8 (7.9–9.7)
Wave Direction (degrees clockwise from North)	December–March	50 (330–90)	50 (330–100)	110 (80–130)
	June–September	100 (30–240)	110 (70–200)	150 (140–160)
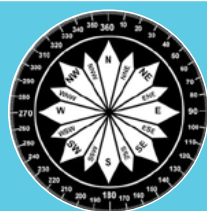
Mean annual cycle of wave height and mean wave direction (hindcast)
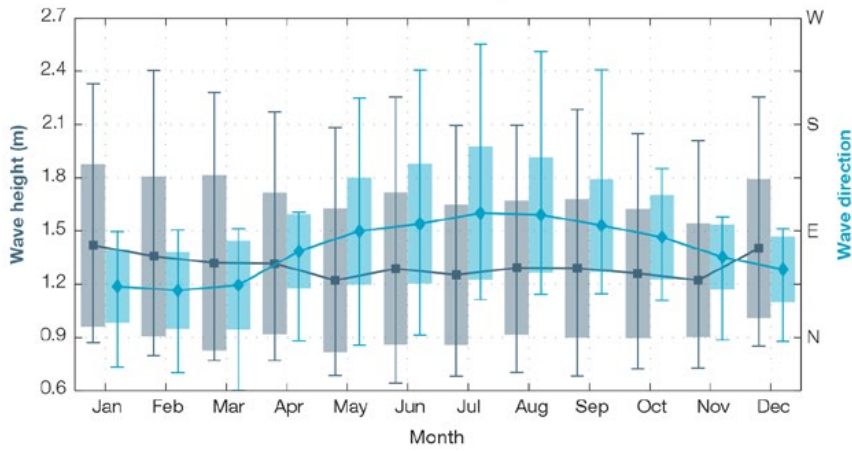Nuku'alofa, Tonga

Figure 14.1: Mean annual cycle of wave height (grey) and mean wave direction (blue) at Nuku'alofa in hindcast data (1979–2009). To give an indication of interannual variability of the monthly means of the hindcast data, shaded boxes show 1 standard deviation around the monthly means, and error bars show the 5–95% range. The direction from which the waves are travelling is shown (not the direction towards which they are travelling).

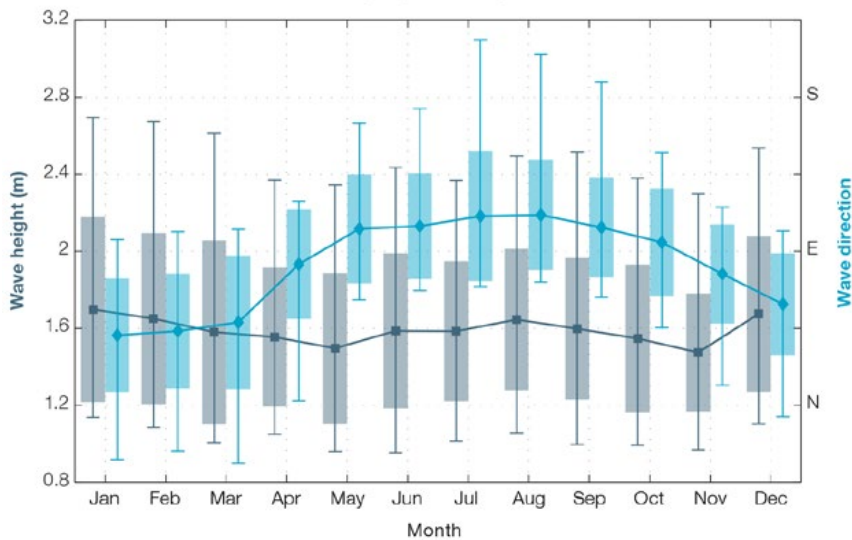Mean annual cycle of wave height and mean wave direction (hindcast)
Lupepau'u, Tonga

Figure 14.2: Mean annual cycle of wave height (grey) and mean wave direction (blue) at Lupepau'u in hindcast data (1979–2009). To give an indication of interannual variability of the monthly means of the hindcast data, shaded boxes show 1 standard deviation around the monthly means, and error bars show the 5–95% range. The direction from which the waves are travelling is shown (not the direction towards which they are travelling).

14.4 Observed Trends

14.4.1 Air Temperature

Annual and Half-year Mean Air Temperature

Annual and November–April mean and minimum temperatures have increased at Nuku'alofa since 1949 (Figure 14.3 and Table 14.2). Maximum, minimum and mean temperatures have increased in the November–April period. Minimum temperatures have increased in the May–October period.

Annual temperature trends are not available for Lupepau'u due to insufficient data. May–October trends are presented with maximum temperature trends for November–April. These trends are mostly positive. A statistically significant (5% level) cooling trend is present in minimum temperature data during May–October at Lupepau'u. This is likely due to underlying data issues including missing data throughout the record,

particularly in the last decade, and/or the extension of the Lupepau'u record with data from the Vava'u observation site which is on the opposite side of the island (Figure 14.4).
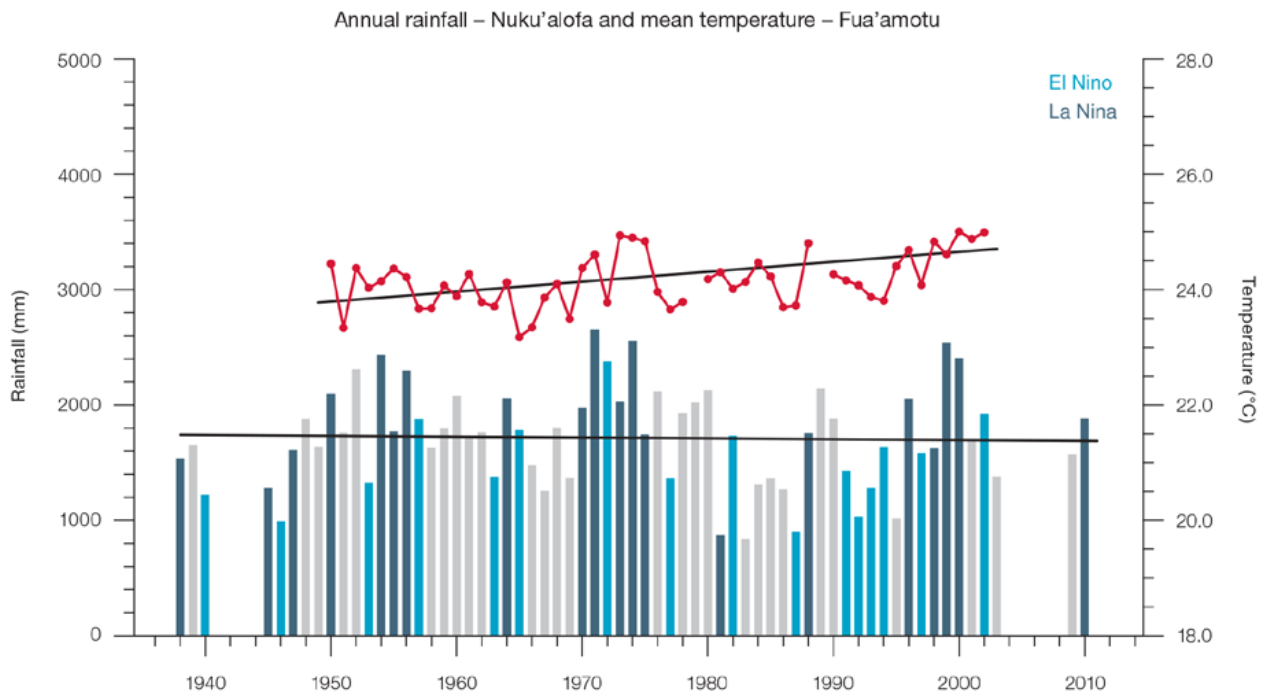

Figure 14.3: Observed time series of annual average values of mean air temperature (red dots and line) and total rainfall (bars) at Nuku'alofa. Light blue, dark blue and grey bars denote El Niño, La Niña and neutral years respectively. Solid black trend lines indicate a least squares fit.

Figure 14.4: Observed time series of annual average values of mean air temperature (red dots and line) and total rainfall (bars) at Lupepau'u. Light blue, dark blue and grey bars denote El Niño, La Niña and neutral years respectively. Solid black trend lines indicate a least squares fit.
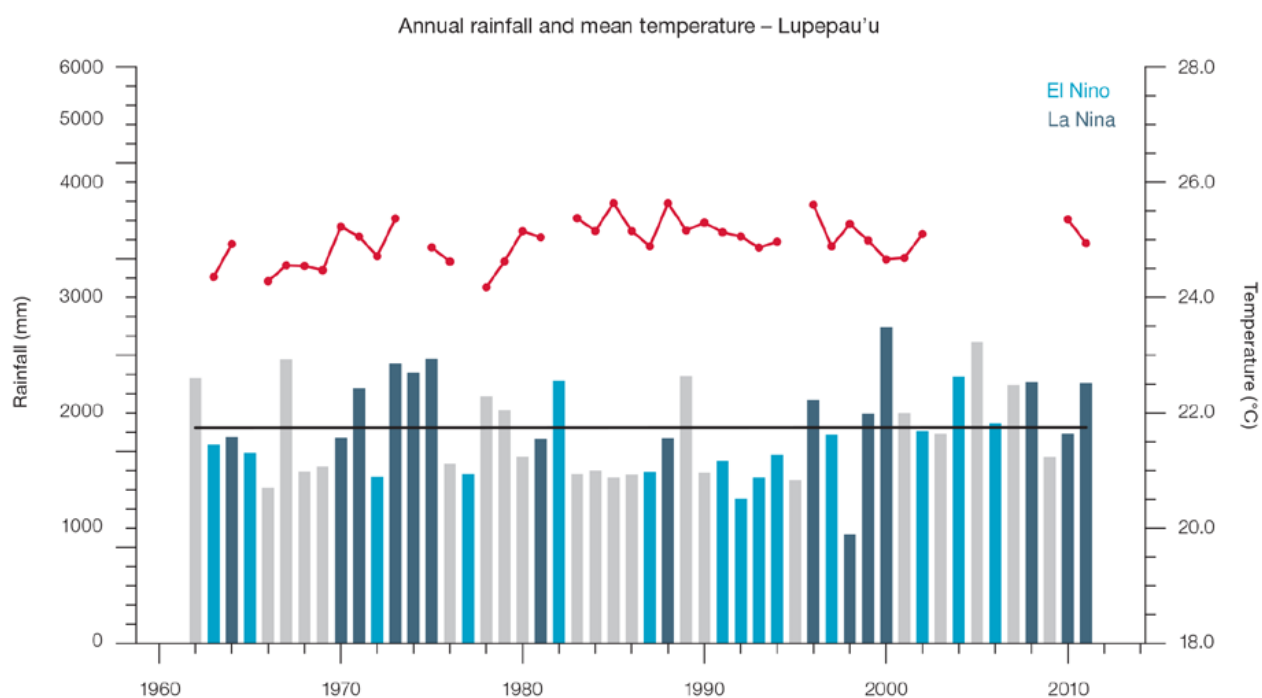
Table 14.2: Annual and half-year trends in air temperature and rainfall at Nuku'alofa (top) and Lupepau'u (bottom). The 95% confidence intervals are shown in brackets. Values for trends significant at the 5% level are shown in **boldface**.

Nuku'alofa	Tmax (°C/10yrs)	Tmin (°C/10yrs)	Tmean (°C/10yrs)	Total Rain (mm/10yrs)
		1949–2011		1938–2011
Annual	+0.08 (0.00, +0.17)	**+0.20** (+0.08, +0.30)	**+0.14** (+0.04, +0.23)	-20.1 (-103.9, +67.0)
Nov-Apr	**+0.15** (+0.06, +0.22)	**+0.29** (+0.16, +0.4)	**+0.22** (+0.1, +0.23)	-14.3 (-74.8, +50.2)
May-Oct	+0.03 (-0.017 +0.13)	**+0.13** (+0.01, +0.25)	+0.07 (-0.03, +0.19)	-5.3 (-30.0, +24.0)

Lupepau'u	Tmax (°C /10yrs)	Tmin (°C/10yrs)	Tmean (°C/10yrs)	Total Rain (mm/10yrs)
		1956–2011		1947–2011
Annual	-	-	-	+11.7 (-73.4, +91.1)
Nov–Apr	**+0.40** (+0.14, +0.66)	-	-	-23.1 (-82.8, +38.0)
May–Oct	**+0.35** (+0.17, +0.53)	**-0.16** (-0.31, -0.03)	+0.11 (-0.04, +0.26)	**+38.7** (+0.4, +74.5)

Extreme Daily Air Temperature

There is insufficient daily temperature data to produce trends in temperature extremes for Nuku'alofa. The positive trend in the number of Cool Days at Lupepau'u from 1947 is statistically significant (Table 14.3 and Figure 14.5) but inconsistent with regional and global trends. This is likely due to underlying data issues including missing data in the last decade, but may be related to the extension of the Lupepau'u record with data from the Vava'u observation site which is on the opposite side of the island.

Table 14.3: Annual trends in air temperature and rainfall extremes at Nuku'alofa (left) and Lupepau'u (right). The 95% confidence intervals are shown in brackets. Values for trends significant at the 5% level are shown in **boldface**. A dash (-) indicates insufficient data for calculating trends.

	Nuku'alofa	Lupepau'u
TEMPERATURE		**1957–2011**
Warm Days (days/decade)	-	+8.27 (0.00, +16.17)
Warm Nights (days/decade)	-	-
Cool Days (days/decade)	-	**-14.26** (-20.83, -7.64)
Cool Nights (days/decade)	-	-
RAINFALL	**1971–2011**	**1947–2011**
Rain Days ≥ 1 mm (days/decade)	-0.47 (-9.85, +11.16)	+0.02 (-4.36, +4.13)
Very Wet Day rainfall (mm/decade)	+79.18 (-38.45, +182.61)	+41.66 (-30.68, +92.23)
Consecutive Dry Days (days/decade)	-1.5 (-4.28, +1.30)	-0.09 (-1.17, +0.91)
Max 1-day rainfall (mm/decade)	+6.89 (-13.11, +24.88)	+0.96 (-6.87, +9.57)

Warm Days: Number of days with maximum temperature greater than the 90th percentile for the base period 1971–2000
Warm Nights: Number of days with minimum temperature greater than the 90th percentile for the base period 1971–2000
Cool Days: Number of days with maximum temperature less than the 10th percentile for the base period 1971–2000
Cool Nights: Number of days with minimum temperature less than the 10th percentile for the base period 1971–2000
Rain Days ≥ 1 mm: Annual count of days where rainfall is greater or equal to 1 mm (0.039 inches)
Very Wet Day rainfall: Amount of rain in a year where daily rainfall is greater than the 95th percentile for the reference period 1971–2000
Consecutive Dry Days: Maximum number of consecutive days in a year with rainfall less than 1 mm (0.039 inches)
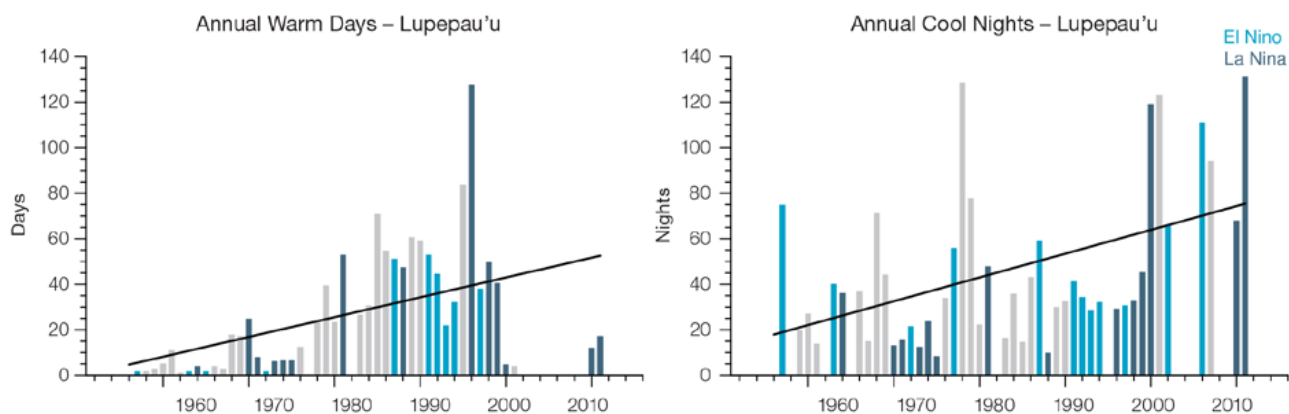Max 1-day rainfall: Annual maximum 1-day rainfall

Figure 14.5: Observed time series of annual total number of Warm Days (left) and annual Cool Nights (right) at Lupepau'u. Solid black trend line indicates a least squares fit.

14.4.2 Rainfall

Annual and Half-year Total Rainfall

Notable interannual variability associated with the ENSO is evident in the observed rainfall record for Nuku'alofa (Figure 14.3) and Lupepau'u (Figure 14.4). The positive trend in Lupepau'u May–October rainfall (dry season; Table 14.2) is statistically significant at the 5% level. This trend may be associated with the mean location of the SPCZ either being displaced towards Tonga and/or there being a change in the intensity of rainfall associated with the SPCZ. Tonga's rainfall is influenced by the position and strength of the SPCZ which lies between Samoa and Tonga between November and April (wet season). From May–October, the SPCZ is normally to the north-east

of Samoa, often weak, inactive and sometimes non-existent. Another possibility may be an increase in the amount of rainfall that is associated with the southerly trade winds. Tonga is usually within the trade wind zone between May and October. The other total rainfall trends presented in Table 14.2, Figure 14.3 and 14.4 are not statistically significant. In other words, excluding Lupepau'u dry season rainfall, the other trends show little change at Nuku'alofa and Lupepau'u.

Daily Rainfall

Daily rainfall trends for Nuku'alofa and Lupepau'u are presented in Table 14.3. Due to large year-to-year variability, there are no significant trends in the daily rainfall indices. Figure 14.6 shows insignificant trends in the annual Very Wet Days and Max 1-day rainfall at both sites.

14.4.3 Tropical Cyclones

When tropical cyclones affect Tonga they tend to do so between November and April. Occurrences outside this period are rare. The tropical cyclone archive for the Southern Hemisphere indicates that between the 1969/70 and 2010/11 seasons 85 tropical cyclones developed within or crossed the Tonga EEZ. This represents an average of 20 cyclones per decade. Refer to Chapter 1, Section 1.4.2 (Tropical Cyclones) for an explanation of the difference in the number of tropical cyclones occurring in Tonga in this report (Australian Bureau of Meteorology and CSIRO, 2014) compared to Australian Bureau of Meteorology and CSIRO (2011).

The interannual variability in the number of tropical cyclones in Tonga EEZ is large, ranging from zero in some seasons to five in 1979/80, 1992/93
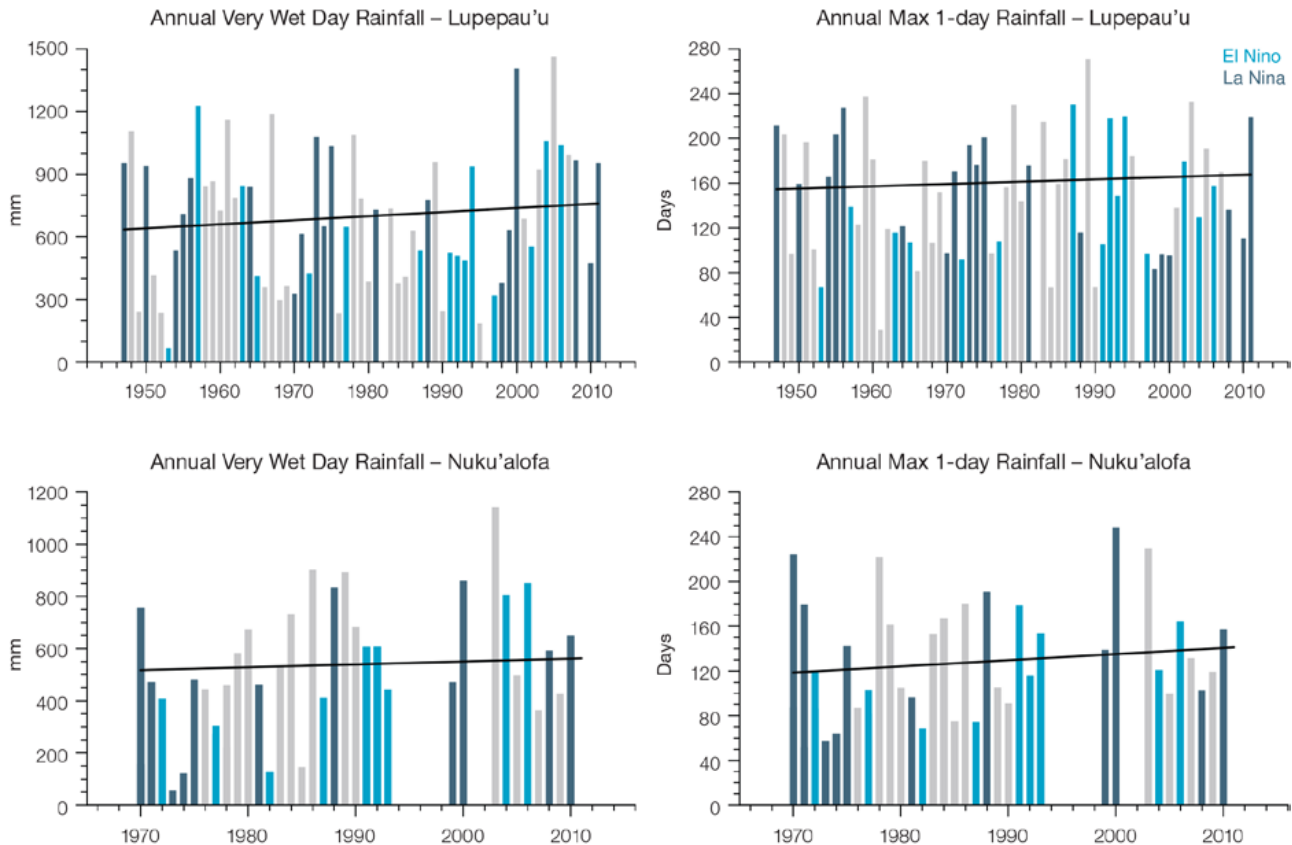

Figure 14.6: Observed time series of annual total values of Very Wet Days at Lupepau'u (top left panel) and Nuku'alofa (bottom left panel). Annual Max 1-day rainfall at Lupepau'u (top right panel) and Nuku'alofa (bottom right panel). Solid black trend lines indicate a least squares fit.

and 2002/03 (Figure 14.7). The differences between tropical cyclone average occurrence in El Niño, La Niña and neutral years are not statistically significant. Nineteen of the 55 tropical cyclones (35%) between the 1981/82 and 2010/11 seasons were severe events (Category 3 or stronger) in the Tonga EEZ.

Long term trends in frequency and intensity have not been presented as country scale assessment is not recommended. Some tropical cyclone tracks analysed in this subsection include the tropical depressions stage (sustained winds less than or equal to 34 knots) before and/or after tropical cyclone formation.

Additional information on historical tropical cyclones in the Tonga region can be found at www.bom.gov.au/cyclone/history/tracks/index.shtml
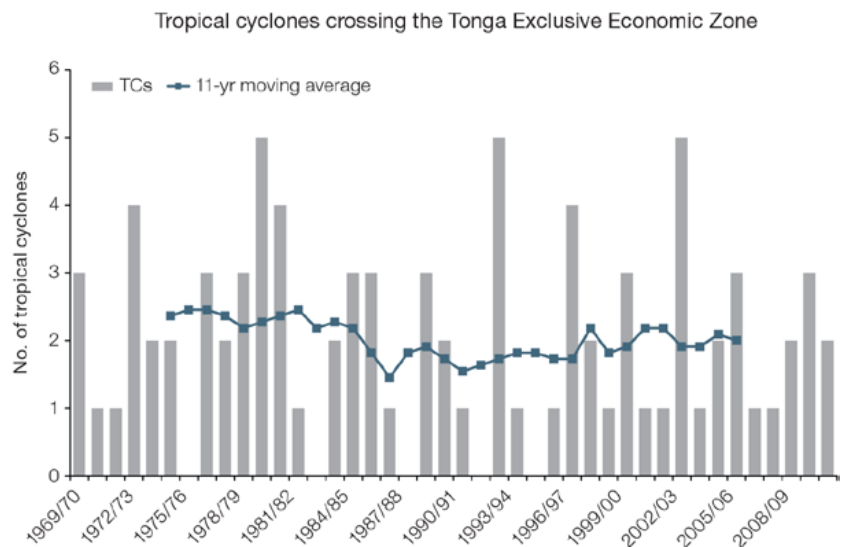

Figure 14.7: Time series of the observed number of tropical cyclones developing within and crossing the Tonga EEZ per season. The 11-year moving average is in blue.

14.5 Climate Projections

The performance of the available Coupled Model Intercomparison Project (Phase 5) (CMIP5) climate models over the Pacific has been rigorously assessed (Brown et al., 2013a, b; Grose et al., 2014; Widlansky et al., 2013). The simulation of the key processes and features for Tonga region is similar to the previous generation of CMIP3 models, with all the same strengths and many of the same weaknesses. The best-performing CMIP5 models used here have lower biases (differences between the simulated and observed climate data) than the best CMIP3 models, and there are fewer poorly-performing models. For Tonga, the most important model bias is that the rainfall maximum of the SPCZ is too zonally (east-west) oriented and the rainfall region to the south of Tonga, especially in Southern Hemisphere winter, is not simulated by most models. This lowers confidence in the model projections. Out of 27 models assessed, three models were rejected for use in these projections due to biases in the mean climate and in the simulation of the SPCZ. Climate projections have been derived from up to 24 new GCMs in the CMIP5 database (the exact number is different for each scenario, Appendix A), compared with up to 18 models in the CMIP3 database reported in Australian Bureau of Meteorology and CSIRO (2011).

It is important to realise that the models used give different projections under the same scenario. This means there is not a single projected future for Tonga, but rather a range of possible futures for each emission scenario.

This range is described below. 14.5.1 Temperature

Further warming is expected over Tonga (Figure 14.8, Table 14.6). Under all RCPs, the warming is up to 1.0°C by 2030, relative to 1995, but after 2030 there is a growing difference in warming between each RCP. In Tonga by 2090, RCP8.5 results in a warming of 1.8–4.1°C while RCP2.6 gives a warming of 0.2–1.1°C. The total range of projected temperatures is broader than that presented in Australian Bureau of Meteorology and CSIRO (2011) because a wider range of emissions scenarios is considered. While relatively warm and cool years and decades will still occur due to natural variability, there is projected to be more warm years and decades on average in a warmer climate.
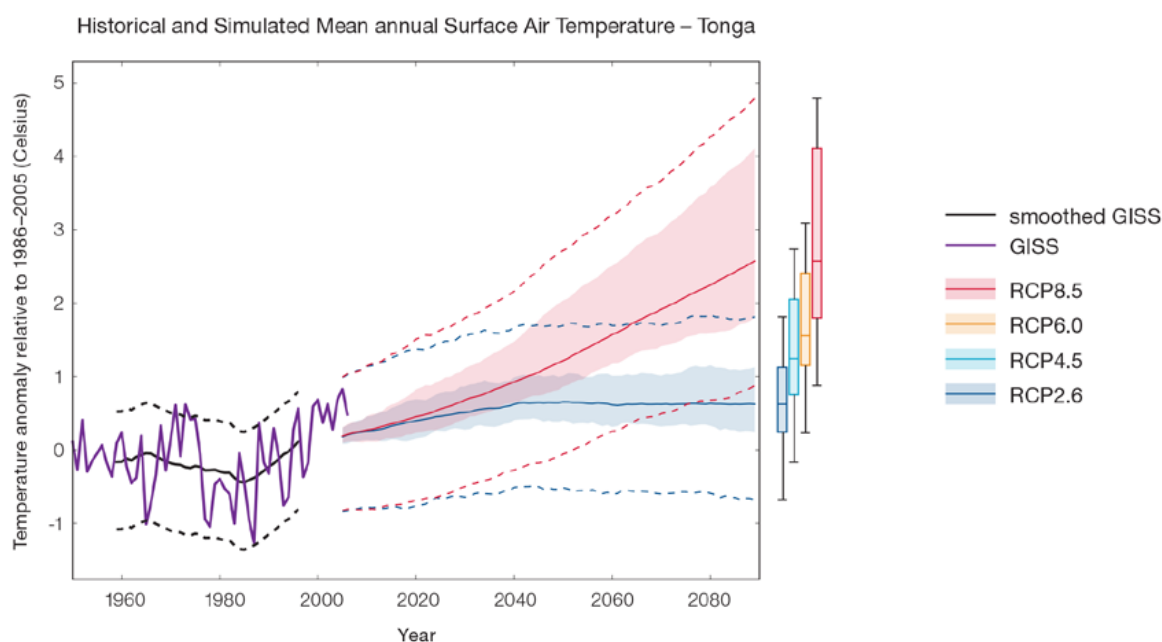
Historical and Simulated Mean annual Surface Air Temperature – Tonga

Figure 14.8: Historical and simulated surface air temperature time series for the region surrounding Tonga. The graph shows the anomaly (from the base period 1986–2005) in surface air temperature from observations (the GISS dataset, in purple), and for the CMIP5 models under the very high (RCP8.5, in red) and very low (RCP2.6, in blue) emissions scenarios. The solid red and blue lines show the smoothed (20-year running average) multi-model mean anomaly in surface air temperature, while shading represents the spread of model values (5–95th percentile). The dashed lines show the 5–95th percentile of the observed interannual variability for the observed period (in black) and added to the projections as a visual guide (in red and blue). This indicates that future surface air temperature could be above or below the projected long-term averages due to interannual variability. The ranges of projections for a 20-year period centred on 2090 are shown by the bars on the right for RCP8.5, 6.0, 4.5 and 2.6.

There is *very high confidence* that temperatures will rise because:

- It is known from theory and observations that an increase in greenhouse gases will lead to a warming of the atmosphere; and
- Climate models agree that the long-term average temperature will rise.

There is *medium confidence* in the model average temperature change shown in Table 14.6 because the new models do a good job of simulating the rate of temperature change of the recent past.

14.5.2 Rainfall

The CMIP5 models show a range of projected annual rainfall change from an increase to a decrease, and the model average is for a slight increase. There is a range of results from the different models under each scenario, with the largest range of uncertainty for the higher emission scenario by the end of the century (Figure 14.9, Table 14.6). Similar to the CMIP3 results, around two-thirds of models simulate increased rainfall in November–April, but there is less agreement on the direction of changes in May–October rainfall. Mean rainfall increased in Tonga between 1979 and 2006 (Figure 14.9), but the models do not project this will continue at

the same rate into the future. This indicates that the recent increase may be partly caused by natural variability, not entirely by global warming. It is also possible that the models do not simulate a key process driving the recent change. However, the recent change is not particularly large (<10%) and the observed record shown is not particularly long (28 years), so it is difficult to determine the significance of this difference, and its cause. The year-to-year rainfall variability over Tonga is much larger than the projected change, except in the highest emission scenario by 2090. There will still be wet and dry years and decades due to natural variability, but models show that the long-term average may be wetter or drier by the end of the century under the high scenario.
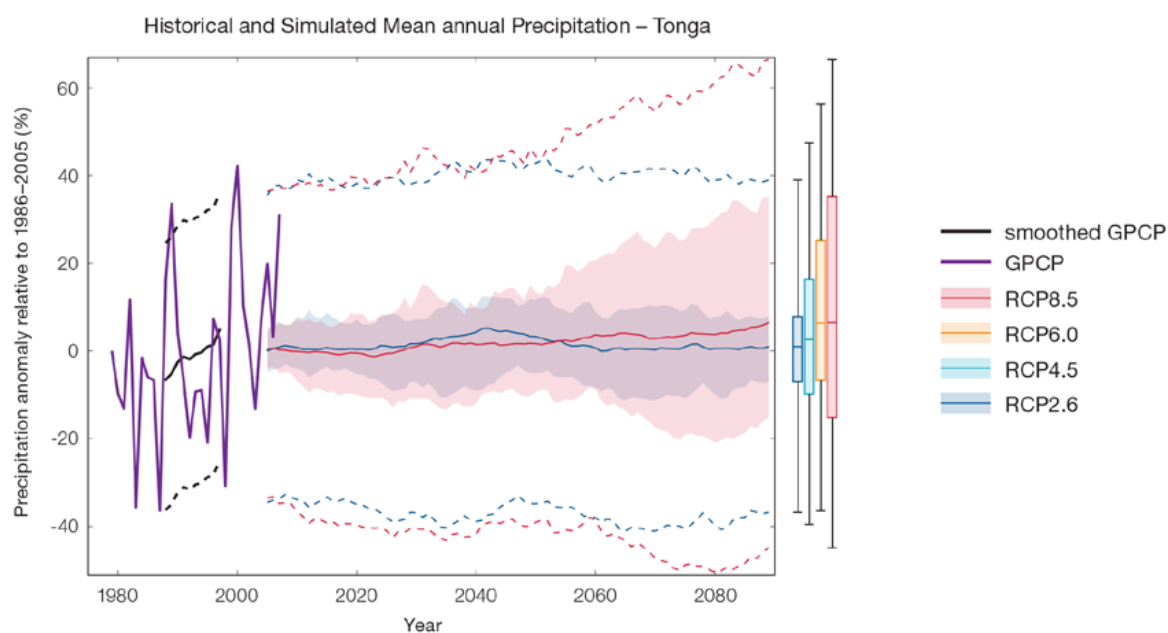
Figure 14.9: Historical and simulated annual average rainfall time series for the region surrounding Tonga. The graph shows the anomaly (from the base period 1986–2005) in rainfall from observations (the GPCP dataset, in purple), and for the CMIP5 models under the very high (RCP8.5, in red) and very low (RCP2.6, in blue) emissions scenarios. The solid red and blue lines show the smoothed (20-year running average) multi-model mean anomaly in rainfall, while shading represents the spread of model values (5–95th percentile). The dashed lines show the 5–95th percentile of the observed interannual variability for the observed period (in black) and added to the projections as a visual guide (in red and blue). This indicates that future rainfall could be above or below the projected long-term averages due to interannual variability. The ranges of projections for a 20-year period centred on 2090 are shown by the bars on the right for RCP8.5, 6.0, 4.5 and 2.6.

Although the average of models shows a slight increase in rainfall, there is no strong agreement as to the direction of change in the models. This lowers the confidence of the projected changes, and makes the amount difficult to determine. The 5–95th percentile range of projected values from CMIP5 climate models is large for RCP8.5 (very high emissions): -11 to +10% by 2030 and -15 to +35% by 2090.

There is *low confidence* that annual rainfall over Tonga will increase slightly in the long-term, because:

- There are a range of different results from the models from an increase to a decrease, especially for the high emission scenario, and many models project little change; and

- Changes in the SPCZ rainfall are uncertain. The majority of CMIP5 models simulate increased rainfall in the western part of the SPCZ (Brown et al., 2013a) and decreased rainfall in the eastern part of the SPCZ, however rainfall changes are sensitive to sea-surface temperature gradients, which are not well simulated in many models (Widlansky et al., 2013). See Box in Chapter 1 for more details.

There is *low confidence* in the model average rainfall change shown in Table 14.6 because:

- The complex set of processes involved in tropical rainfall is challenging to simulate in models.

This means that the confidence in the projection of rainfall is generally lower than for other variables such as temperature;

- There is a different magnitude of change in the SPCZ rainfall projected by models that have reduced sea-surface temperature biases (Australian Bureau of Meteorology and CSIRO, 2011, Chapter 7 (downscaling); Widlanksy et al., 2012) compared to the CMIP5 models; and

- The future behaviour of the ENSO is unclear, and the ENSO strongly influences year-to-year rainfall variability.

14.5.3 Extremes

Extreme Temperature

The temperature on extremely hot days is projected to increase by about the same amount as average temperature. This conclusion is based on analysis of daily temperature data from a subset of CMIP5 models (Chapter 1). The frequency of extremely hot days is also expected to increase.

The temperature of the 1-in-20-year hot day is projected to increase by approximately 0.6°C by 2030 under the RCP2.6 scenario and by 7°C under the RCP8.5 scenario. By 2090 the projected increase is 0.7°C for RCP2.6 and 3°C for RCP8.5.

There is *very high confidence* that the temperature of extremely hot days and the temperature of extremely cool days will increase, because:

- A change in the range of temperatures, including the extremes, is physically consistent with rising greenhouse gas concentrations;
- This is consistent with observed changes in extreme temperatures around the world over recent decades (IPCC, 2012); and
- All the CMIP5 models agree on an increase in the frequency and intensity of extremely hot days and a decrease in the frequency and intensity of cool days;

There is *medium confidence* in the magnitude of projected change in extreme temperature because models generally underestimate the current intensity and frequency of extreme events. Changes to the particular driver of extreme temperatures affect whether the change to extremes is more or less than the change in the average temperature, and the changes to the drivers of extreme temperatures in Tonga are currently unclear.

Extreme Rainfall

The frequency and intensity of extreme rainfall events are projected to increase. This conclusion is based on analysis of daily rainfall data from a subset of CMIP5 models using a similar method to that in Australian Bureau of Meteorology and CSIRO (2011) with some improvements (Chapter 1), so the results are slightly different to those in Australian Bureau of Meteorology and CSIRO (2011). The current 1-in-20-year daily rainfall amount is projected to increase by approximately 7 mm by 2030 for RCP2.6 and by 4 mm by 2030 for RCP8.5. By 2090, it is projected to increase by approximately 5 mm for RCP2.6 and by 36 mm for RCP8.5. The majority of models project the current 1-in-20-year daily rainfall event will become, on average, a 1-in-9-year event for RCP2.6 and a 1-in-5-year event for RCP8.5 by 2090. These results are different to those found in Australian Bureau of Meteorology and CSIRO (2011) because of different methods used (Chapter 1).

There is *high confidence* that the frequency and intensity of extreme rainfall events will increase because:

- A warmer atmosphere can hold more moisture, so there is greater potential for extreme rainfall (IPCC, 2012);
- Consistent with the mixed changes in mean and extreme rainfall indices, the pattern of change in the extreme rainfalls shows considerable variation from station to station. For the lower recurrence intervals (2 and 5 years) there is little systematic change in rainfall intensity. In some contrast the very most extreme rainfall being that occurring with an average recurrence interval of 20 years shows a mean increase of 3.5%, (significant at the 10% level);

- Increases in extreme rainfall in the Pacific are projected in all available climate models; and
- An increase in extreme rainfall events within the SPCZ region was found by an in-depth study of extreme rainfall events in the SPCZ (Cai et al., 2012).

There is *low confidence* in the magnitude of projected change in extreme rainfall because:

- Models generally underestimate the current intensity of local extreme events;
- The simulation of extreme events in Tonga is influenced by the SPCZ biases;
- Changes in extreme rainfall projected by models may be underestimated because models seem to underestimate the observed increase in heavy rainfall with warming (Min et al., 2011);
- GCMs have a coarse spatial resolution, so they do not adequately capture some of the processes involved in extreme rainfall events; and
- The Conformal Cubic Atmospheric Model (CCAM) downscaling model has finer spatial resolution and the CCAM results presented in Australian Bureau of Meteorology and CSIRO (2011) indicates a smaller increase in the number of extreme rainfall days, and there is no clear reason to accept one set of models over another.

Drought

Drought projections (defined in Chapter 1) are described in terms of changes in proportion of time in drought, frequency and duration by 2090 for very low and very high emissions (RCP2.6 and 8.5).

For Tonga the overall proportion of time spent in drought is expected to decrease slightly under all scenarios. These results are different to those in Australian Bureau of Meteorology and CSIRO (2011), which reported little change in drought. Under RCP8.5 the frequency and duration of drought in all categories is projected to decrease slightly (Figure 14.10). Under RCP2.6 the frequency and duration of severe and extreme drought events is expected to decrease slightly while the frequency and duration of mild and moderate drought events is projected to stay approximately the same.

There is *low confidence* in this direction of change because:

- There is only *low confidence* in the direction of mean rainfall change;
- These drought projections are based upon a subset of models; and
- Like the CMIP3 models, the majority of the CMIP5 models agree on this direction of change.

There is *low confidence* in the projections of drought duration and frequency because there is *low confidence* in the magnitude of rainfall projections, and no consensus about projected changes in the ENSO, which directly influence the projection of drought.

Tropical Cyclones

Global Picture

There is a growing level of consistency between models that on a global basis the frequency of tropical cyclones is likely to decrease by the end of the 21st century. The magnitude of the decrease varies from 6% to35 % depending on the modelling study. There is also a general agreement between models that there will be an increase in the mean maximum wind speed of cyclones by between 2% and 11% globally, and an increase in rainfall rates of the order of 20% within 100 km of the cyclone centre (Knutson et al., 2010). Thus, the scientific community has a *medium* level of confidence in these global projections.
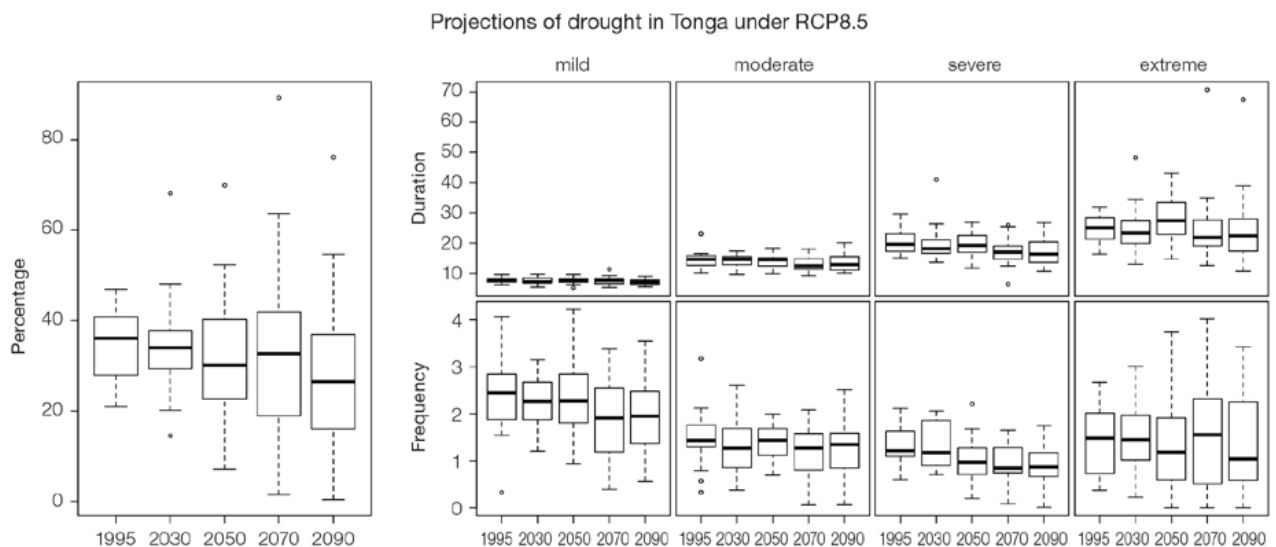
Figure 14.10: Box-plots showing percent of time in moderate, severe or extreme drought (left hand side), and average drought duration and frequency for the different categories of drought (mild, moderate, severe and extreme) for Tonga. These are shown for 20-year periods centred on 1995, 2030, 2050, 2070 and 2090 for the RCP8.5 (very high emissions) scenario. The thick dark lines show the median of all models, the box shows the interquartile (25–75%) range, the dashed lines show 1.5 times the interquartile range and circles show outlier results.

Tonga

In Tonga, the projection is for a decrease in cyclone genesis (formation) frequency for the south-east basin (see Figure 14.11 and Table 14.4). The confidence level for this projection is high. The GCMs show consistent results across models for changes in cyclone frequency for the south-east basin, using the direct detection methodologies (OWZ or CDD) described in Chapter 1. Approximately 80% of the projected changes, based on these methods, vary between a 5% decrease to a 50% decrease in genesis frequency with half projecting a decrease between 20 and 40%. The empirical techniques assess changes in the main atmospheric ingredients known to be necessary for cyclone formation. Projections based upon these techniques suggest the conditions for cyclone formation will become less favourable in this region with about half of projected changes indicating decreases between 10 and 40% in genesis frequency. These projections are consistent with those of Australian Bureau of Meteorology and CSIRO (2011).

Table 14.4: Projected percentage change in cyclone frequency in the south-east basin (0–40°S; 170°E–130°W) for 22 CMIP5 climate models, based on five methods, for 2080–2099 relative to 1980–1999 for RCP8.5 (very high emissions). The 22 CMIP5 climate models were selected based upon the availability of data or on their ability to reproduce a current-climate tropical cyclone climatology (See Section 1.5.3 – Detailed Projection Methods, Tropical Cyclones). Blue numbers indicate projected decreases in tropical cyclone frequency, red numbers an increase. MMM is the multi-model mean change. N increase is the proportion of models (for the individual projection method) projecting an increase in cyclone formation.

| Model	GPI change	GPI-M change	Tippett	CDD	OWZ
access10	5	-22	-54	-23	
access13	-26	-26	-36	-10	
bcccsm11	-3	-1	-28		-5
canesm2	-7	-13	-49	-6	
ccsm4				-78	-5
cnrm_cm5	-4	-5	-26	8	7
csiro_mk36	-16	-13	-33	-26	-27
fgoals_g2	6	-8	-40		
fgoals_s2	-15	-20	-48		
gfdl_esm2m				-48	-36
gfdl_cm3	-1	-5	-25		-11
gfdl_esm2g				-18	-36
gisse2r	17	16	-6		
hadgem2_es	-8	-11	-51		
lnm	-3	-3	-30		
ipslcm5alr	-13	-19	-43		
ipslcm5blr				7	
miroc5				-43	-22
mirocesm	-40	-38	46		
mpim	-26	-19	-41		
mricgcm3	-8	-10	-28		
noresm1m	-36	-40	-59	-80	
MMM	-11	-14	-32	-29	-17
N increase	0.2	0.1	0.1	0.2	0.125
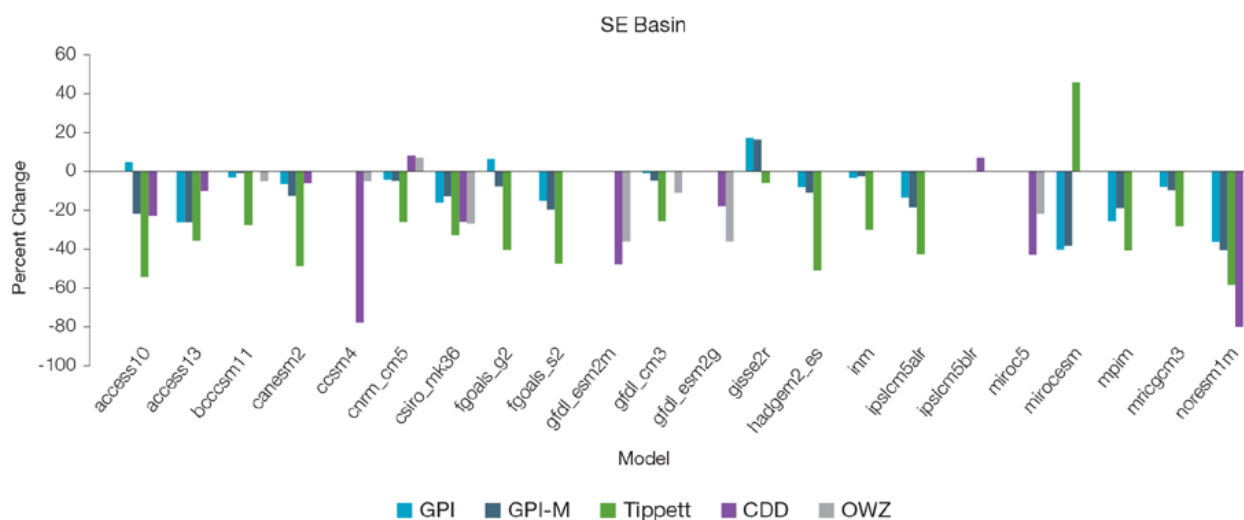
Figure 14.11: Projected percentage change in cyclone frequency in the south-east basin (data from Table 14.4).

14.5.4 Coral Reefs and Ocean Acidification

As atmospheric CO_2 concentrations continue to rise, oceans will warm and continue to acidify. These changes will impact the health and viability of marine ecosystems, including coral reefs that provide many key ecosystem services (*high confidence*). These impacts are also likely to be compounded by other stressors such as storm damage, fishing pressure and other human impacts.

The projections for future ocean acidification and coral bleaching use three RCPs (2.6, 4.5, and 8.5).

Ocean Acidification

Ocean acidification is expressed in terms of aragonite saturation state (Chapter 1). In Tonga the aragonite saturation state has declined from about 4.5 in the late 18th century to an observed value of about 4.0±0.1 by 2000 (Kuchinke et al., 2014). All models show that the aragonite saturation state, a proxy for coral reef growth rate, will continue to decrease as atmospheric CO_2 concentrations increase (*very high confidence*). Projections from CMIP5 models indicate that under RCPs 8.5 and 4.5 the median aragonite saturation state will transition to marginal conditions (3.5) around 2030. In RCP8.5 the aragonite saturation state continues to strongly decline thereafter to values

where coral reefs have not historically been found (< 3.0). Under RCP4.5 the aragonite saturation plateaus around 3.2 i.e. marginal conditions for healthy coral reefs. While under RCP2.6 the median aragonite saturation state never falls below 3.5, and increases slightly toward the end of the century (Figure 14.12) suggesting that the conditions remains adequate for healthy corals reefs. There is *medium confidence* in this range and distribution of possible futures because the projections are based on climate models that do not resolve the reef scale that can play a role in modulating large-scale changes. The impacts of ocean acidification are also likely to affect the entire marine ecosystem impacting the key ecosystem services provided by reefs.
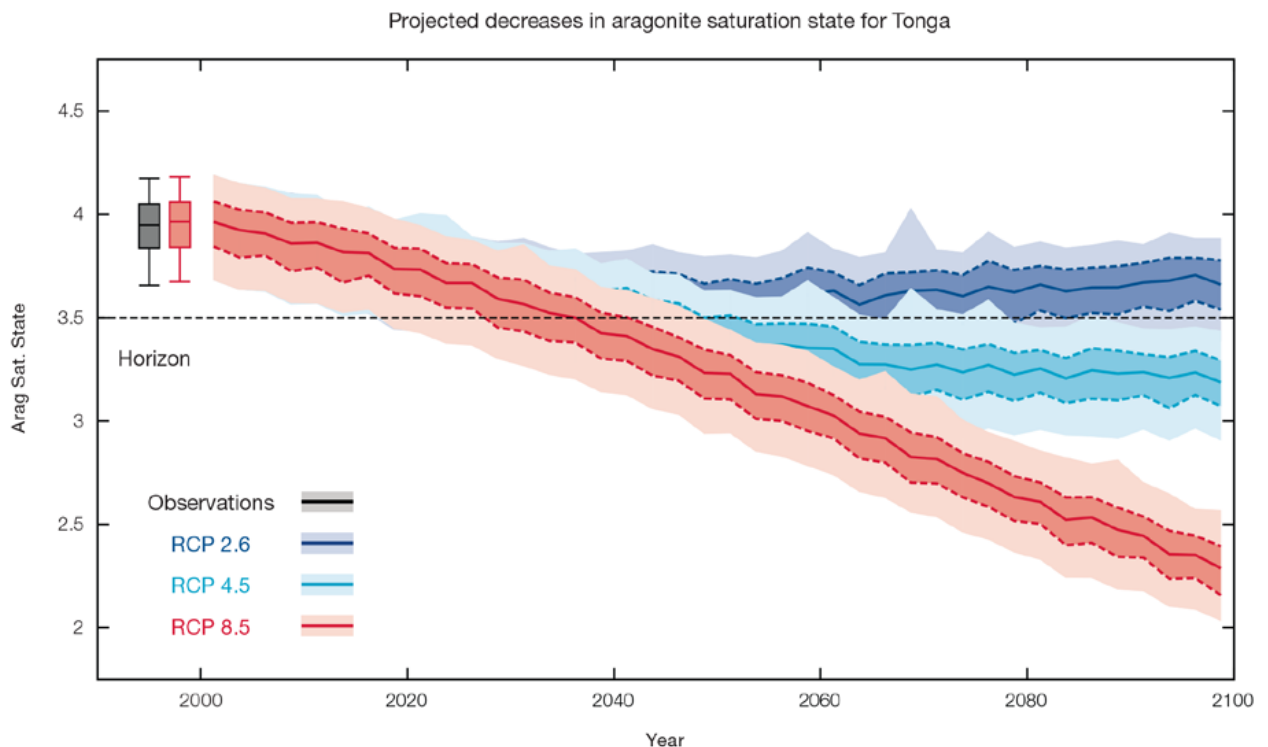

Figure 14.12: Projected decreases in aragonite saturation state in Tonga from CMIP5 models under RCP2.6, 4.5 and 8.5. Shown are the median values (solid lines), the interquartile range (dashed lines), and 5% and 95% percentiles (light shading). The horizontal line represents the transition to marginal conditions for coral reef health (from Guinotte et al., 2003

Coral Bleaching Risk

As the ocean warms, the risk of coral bleaching increases (*very high confidence*). There is *medium confidence* in the projected rate of change for Tonga because there is *medium confidence* in the rate of change of SST, and the changes at the reef scale (which can play a role in modulating large-scale changes) are not adequately resolved. Importantly, the coral bleaching risk calculation does not account the impact of other potential stressors (Chapter 1).

The changes in the frequency (or recurrence) and duration of severe bleaching risk are quantified for different projected SST changes (Table 14.5). Overall there is a decrease in the time between two periods of elevated risk and an increase in the duration of the elevated risk. For example, under a long-term mean increase of 1°C (relative to 1982–1999 period), the average period of severe bleaching risk (referred to as a risk event) will last 8.2 weeks (with a minimum duration of 1.8 weeks and a maximum duration of 4.5 months) and the average time between two risks will be 2.6 years (with the minimum recurrence of 4.3 months and a maximum recurrence of 7.4 years). If severe bleaching events occur more often than once every five years, the long-term viability of coral reef ecosystems becomes threatened.

14.5.5 Sea Level

Mean sea level is projected to continue to rise over the course of the 21st century. There is very *high confidence* in the direction of change. The CMIP5 models simulate a rise of between approximately 7–18 cm by 2030 (very similar values for different RCPs), with increases of 41–88 cm by 2090 under the RCP8.5 (Figure 14.13 and Table 14.6). There is *medium confidence* in the range mainly because there is still uncertainty associated with projections of the Antarctic ice sheet contribution. Interannual variability of sea level will lead to periods of lower and higher regional sea levels. In the past, this interannual variability has been about 18 cm (5–95% range, after removal of the seasonal signal, see dashed lines in Figure 14.13 (a) and it is likely that a similar range will continue through the 21st century.

Table 14.5: Projected changes in severe coral bleaching risk for the Tonga EEZ for increases in SST relative to 1982–1999.

Temperature change [1]	Recurrence interval [2]	Duration of the risk event [3]
Change in observed mean	30 years	6.4 weeks
+0.25°C	24.8 years (23.2 years – 26.3 years)	5.9 weeks (5.3 weeks – 6.6 weeks)
+0.5°C	15.1 years (10.0 years – 19.9 years)	6.5 weeks (4.5 weeks – 8.1 weeks)
+0.75°C	6.3 years (1.5 years – 12.8 years)	8.6 weeks (3.6 weeks – 2.8 months)
+1°C	2.9 years (7.9 months – 7.7 years)	9.0 weeks (2.6 weeks – 3.8 months)
+1.5°C	1.0 years (4.7 months – 2.4 years)	2.8 months (3.3 weeks – 5.1 months)
+2°C	8.8 months (6.0 months – 1.6 years)	4.1 months (6.3 weeks – 6.1 months)

[1] This refers to projected SST anomalies above the mean for 1982–1999.
[2] Recurrence is the mean time between severe coral bleaching risk events. Range (min – max) shown in brackets.
[3] Duration refers to the period of time where coral are exposed to the risk of severe bleaching. Range (min – max) shown in brackets.

Observed and projected relative sea-level change near Tonga

(a)

Tonga
— Reconstruction
— Satellite altimeter
— Tide gauges (3)

Projections
■ RCP8.5
■ RCP6.0
■ RCP4.5
■ RCP2.6

(b) RCP4.5: 2090

14.5.6 Wind-driven Waves

During December–March, there are no significant projected changes in wave properties *(low confidence)* (Table 14.7). Suggested changes include a slight decrease in wave height (Figure 14.14) and period. These features are characteristic of a decrease in the strength of prevailing trade winds. No change is projected in the height of larger storm waves though they may be increasingly directed from the north and west, associated with cyclonic activity *(low confidence)*.

In June–September, there are no statistically significant projected changes in wave height or period, but a very small anticlockwise rotation (toward the southeast) is suggested *(low confidence)* (Table 14.7) possibly associated with a shift in trade winds. Non-significant changes include a slight increase in wave height and period. No change is projected in the larger waves *(low confidence)*.

There is *low confidence* in projected changes in the Tongan wind-wave because:

- Projected changes in wave climate are dependent on confidence of projected changes in the ENSO, which is low; and

- The difference between simulated and observed (hindcast) wave data can be larger than the projected wave changes , which further reduces our confidence in projections.
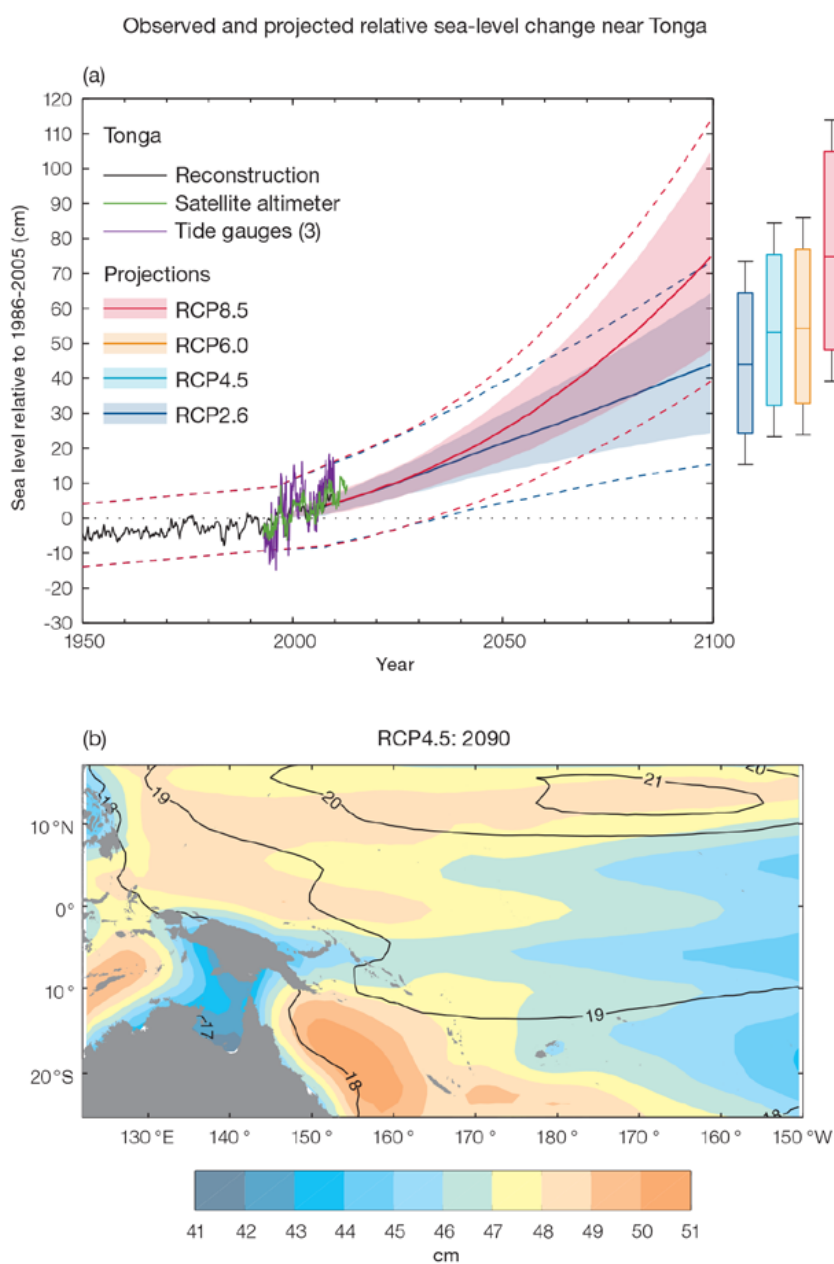
Figure 14.13: (a) The observed tide-gauge records of relative sea-level (since the late 1970s) are indicated in purple, and the satellite record (since 1993) in green. The gridded (reconstructed) sea level data at Tonga (since 1950) is shown in black. Multi-model mean projections from 1995–2100 are given for the RCP8.5 (red solid line) and RCP2.6 emissions scenarios (blue solid line), with the 5–95% uncertainty range shown by the red and blue shaded regions. The ranges of projections for four emission scenarios (RCPs 2.6, 4.5, 6.0 and 8.5) by 2100 are also shown by the bars on the right. The dashed lines are an estimate of interannual variability in sea level (5–95% uncertainty range about the projections) and indicate that individual monthly averages of sea level can be above or below longer-term averages.

(b) The regional distribution of projected sea level rise under the RCP4.5 emissions scenario for 2081–2100 relative to 1986–2005. Mean projected changes are indicated by the shading, and the estimated uncertainty in the projections is indicated by the contours (in cm).

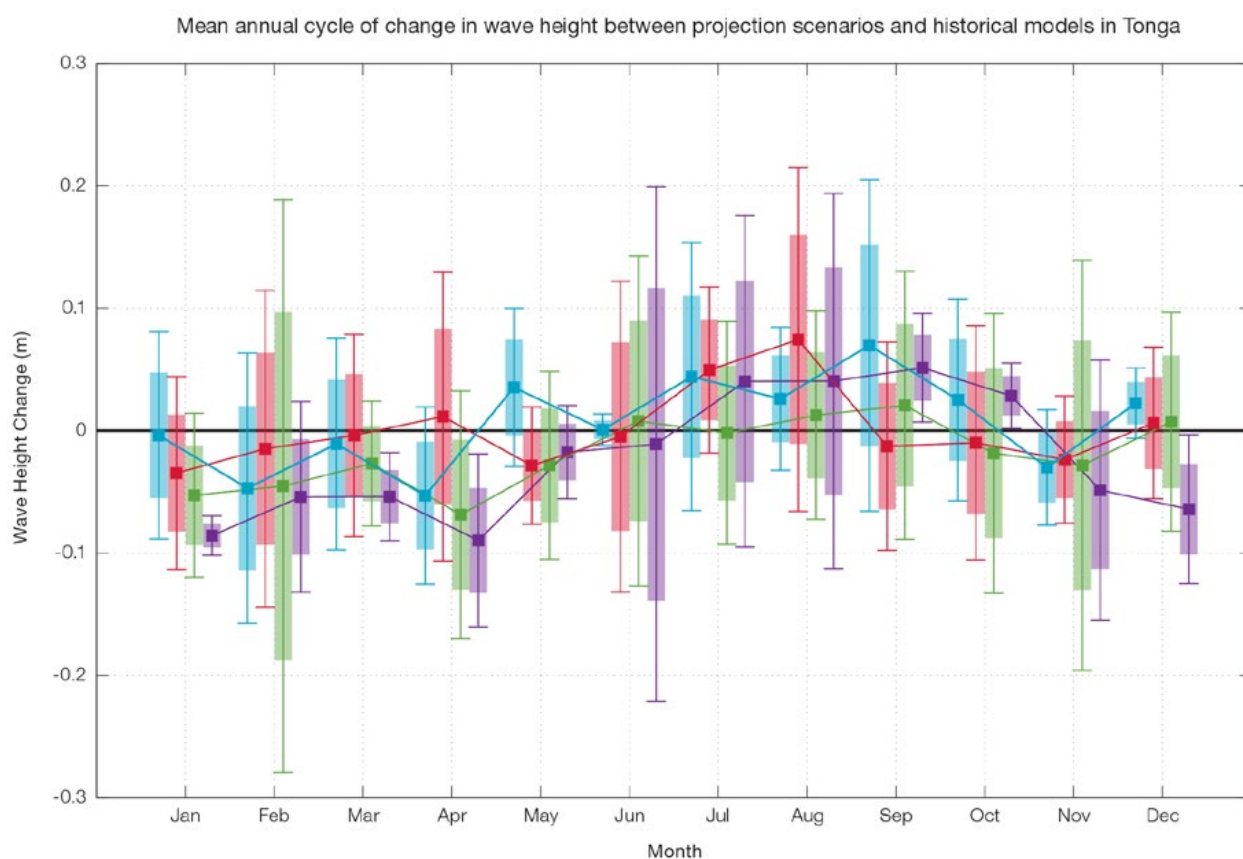Mean annual cycle of change in wave height between projection scenarios and historical models in Tonga

Figure 14.14: Mean annual cycle of change in wave height between projection scenarios and mean of historical models in Tonga. This panel shows a possible small decrease in wave heights in the wet season months (statistically significant in 2090 RCP8.5, very high emissions, in December, January and March), with no change in the dry season months but a suggested increase in wave heights. Shaded boxes show 1 standard deviation of models' means around the ensemble means, and error bars show the 5–95% range inferred from the standard deviation. Colours represent RCP scenarios and time periods: blue 2035 RCP4.5 (low emissions), red 2035 RCP8.5 (very high emissions), green 2090 RCP4.5 (low emissions), purple 2090 RCP8.5 (very high emissions).

14.5.7 Projections Summary

There is *very high confidence* in the direction of long-term change in a number of key climate variables, namely an increase in mean and extremely high temperatures, sea level and ocean acidification. There is *high confidence* that the frequency and intensity of extreme rainfall will increase. There is *low confidence* that mean annual rainfall will increase slightly and the incidence of drought will decrease slightly.

Tables 14.6 and 14.7 quantify the mean changes and ranges of uncertainty for a number of variables, years and emissions scenarios. A number of factors are considered in assessing confidence, i.e. the type, amount, quality and consistency of evidence (e.g. mechanistic understanding, theory, data, models, expert judgment) and the degree of agreement, following the IPCC guidelines (Mastrandrea et al., 2010). Confidence ratings in

the projected magnitude of mean change are generally lower than those for the direction of change (see paragraph above) because magnitude of change is more difficult to assess. For example, there is *very high confidence* that temperature will increase, but *medium confidence* in the magnitude of mean change.

Table 14.6: Projected changes in the annual and seasonal mean climate for Tonga under four emissions scenarios; RCP2.6 (very low emissions, in dark blue), RCP4.5 (low emissions, in light blue), RCP6 (medium emissions, in orange) and RCP8.5 (very high emissions, in red). Projected changes are given for four 20-year periods centred on 2030, 2050, 2070 and 2090, relative to a 20-year period centred on 1995. Values represent the multi-model mean change, with the 5–95% range of uncertainty in brackets. Confidence in the magnitude of change is expressed as *high*, *medium* or *low*. Surface air temperatures in the Pacific are closely related to sea-surface temperatures (SST), so the projected changes to air temperature given in this table can be used as a guide to the expected changes to SST. (See also Section 1.5.2). 'NA' indicates where data are not available.

Variable	Season	2030	2050	2070	2090	Confidence (magnitude of change)
Surface air temperature (°C)	Annual	0.5 (0.3–0.9)	0.6 (0.4–1)	0.6 (0.3–1)	0.6 (0.2–1.1)	*High*
		0.6 (0.3–1)	0.9 (0.6–1.4)	1.1 (0.7–1.8)	1.2 (0.8–2.1)	
		0.5 (0.3–0.8)	0.8 (0.6–1.3)	1.2 (0.8–1.8)	1.6 (1.2–2.4)	
		0.7 (0.4–1)	1.2 (0.8–2)	1.9 (1.4–2.9)	2.6 (1.8–4.1)	
Maximum temperature (°C)	1-in-20 year event	0.6 (0.2–0.9)	0.7 (0.1–1)	0.7 (0–1)	0.7 (-0.1–1.1)	*Medium*
		0.6 (0.2–0.9)	0.9 (0.2–1.2)	1.1 (0.4–1.7)	1.3 (0.6–1.8)	
		NA (NA–NA)	NA (NA–NA)	NA (NA–NA)	NA (NA–NA)	
		0.7 (0.2–1.2)	1.4 (0.7–2)	2.2 (1.3–3)	2.9 (1.7–4.2)	
Minimum temperature (°C)	1-in-20 year event	0.5 (0.1–0.8)	0.6 (0–0.9)	0.7 (0.4–1)	0.6 (0.1–0.9)	*Medium*
		0.6 (0–0.9)	0.9 (0.5–1.3)	1.1 (0.7–1.5)	1.3 (0.7–1.9)	
		NA (NA–NA)	NA (NA–NA)	NA (NA–NA)	NA (NA–NA)	
		0.7 (0.3–1.1)	1.3 (0.7–1.9)	2.1 (1.6–2.7)	2.9 (2.1–4.2)	
Total rainfall (%)	Annual	2 (-7–7)	3 (-5–12)	0 (-11–10)	1 (-7–8)	*Low*
		1 (-12–10)	-1 (-12–10)	2 (-11–18)	3 (-10–16)	
		1 (-8–8)	3 (-8–14)	5 (-8–19)	6 (-7–25)	
		1 (-11–10)	2 (-10–15)	3 (-16–24)	6 (-15–35)	
Total rainfall (%)	Nov-Apr	3 (-9–12)	5 (-6–16)	1 (-11–13)	1 (-11–12)	*Low*
		2 (-14–14)	1 (-13–16)	4 (-10–21)	4 (-9–22)	
		4 (-6–13)	4 (-9–16)	6 (-7–23)	8 (-8–30)	
		2 (-10–12)	3 (-9–18)	6 (-13–35)	11 (-10–53)	
Total rainfall (%)	May-Oct	1 (-8–7)	3 (-5–12)	-1 (-14–8)	1 (-6–10)	*Low*
		0 (-9–9)	-2 (-11–9)	0 (-15–12)	1 (-11–13)	
		-1 (-11–5)	3 (-7–12)	3 (-9–14)	4 (-5–17)	
		0 (-11–12)	0 (-12–11)	-1 (-17–13)	1 (-22–23)	
Aragonite saturation state (Ωar)	Annual	-0.3 (-0.6–0.0)	-0.4 (-0.7--0.1)	-0.4 (-0.7--0.1)	-0.3 (-0.7–0.0)	*Medium*
		-0.3 (-0.6--0.1)	-0.6 (-0.8--0.3)	-0.7 (-1.0--0.4)	-0.8 (-1.0--0.5)	
		NA (NA–NA)	NA (NA–NA)	NA (NA–NA)	NA (NA–NA)	
		-0.4 (-0.7--0.1)	-0.7 (-1.0--0.5)	-1.1 (-1.4--0.9)	-1.5 (-1.8--1.2)	
Mean sea level (cm)	Annual	13 (8–18)	22 (14–30)	31 (19–43)	40 (23–58)	*Medium*
		13 (8–18)	23 (15–31)	35 (22–48)	47 (29–66)	
		12 (7–17)	22 (14–31)	34 (21–47)	48 (30–67)	
		13 (8–18)	25 (17–35)	42 (28–58)	63 (41–88)	

Waves Projections Summary

Table 14.7: Projected average changes in wave height, period and direction in Tonga for December–March and June–September for RCP4.5 (low emissions, in blue) and RCP8.5 (very high emissions, in red), for two 20-year periods (2026–2045 and 2081–2100), relative to a 1986–2005 historical period. The values in brackets represent the 5th to 95th percentile range of uncertainty.

Variable	Season	2035	2090	Confidence (range)
Wave height change (m)	December–March	0.0 (-0.2–0.2) -0.0 (-0.2–0.2)	-0.0 (-0.3–0.2) -0 1 (-0.3–0.1)	*Low*
	June–September	+0.0 (-0.3–0.4) +0.0 (-0.3–0.4)	0.0 (-0.4–0.4) +0.0 (-0.4–0.4)	*Low*
Wave period change (s)	December–March	-0.1 (-1.0–0.9) -0.1 (-1.0–0.8)	-0.1 (-1.2–0.9) -0.1 (-1.3–1.1)	*Low*
	June–September	+0.0 (-0.9–1.0) +0.0 (-0.8–0.9)	+0.0 (-1.1–1.1) 0.0 (-1.2–1.1)	*Low*
Wave direction change (° clockwise)	December–March	-0 (-30–20) 0 (-30–20)	-0 (-30–30) 0 (-30–30)	*Low*
	June–September	0 (-10–10) -0 (-10–10)	0 (-10–10) -5 (-10–5)	*Low*

Wind-wave variables parameters are calculated for a 20-year period centred on 2035.